

## RESEARCH ARTICLE

## PROTOTYPE PHYSICAL MODEL EXPERIMENTAL STUDY ON SHIP ANCHOR IMPACT FOR SUBSEA PIPELINE PROTECTION SYSTEMS

Jiankang Yuan<sup>1</sup>, Chunhong Hu<sup>1</sup>, Yantao Wang<sup>1</sup>, Kunming Ma<sup>1</sup>, Wei Wang<sup>1</sup>, Chunguang Yuan<sup>2\*</sup><sup>1</sup>Offshore Oil Engineering Co., Ltd., Tianjin 300451, China<sup>2</sup>Tianjin Research institute for water transport engineering. M. O. T., Tianjin 300456, China\*Corresponding Author E-mail: [ycgbgg@163.com](mailto:ycgbgg@163.com)

This is an open access article distributed under the Creative Commons Attribution License CC BY 4.0, which permits unrestricted use, distribution, and reproduction in any medium, provided the original work is properly cited.

## ARTICLE DETAILS

## Article History:

Received 20 April 2025  
Accepted 28 May 2025  
Revised 10 June 2025  
Available online 11 June 2025

## ABSTRACT

Subsea pipelines, as critical infrastructure for marine oil and gas transportation, play a key role in the safety of marine environments and resource utilization. However, damage to subsea pipelines caused by activities such as ship anchor dragging is a recurring problem, resulting in significant economic losses. This study investigates the protective effects of subsea pipeline protection systems against anchor dragging through prototype-scale ship anchor impact physical model experiments. By simulating conditions such as the anchor dragging impact, anchor overriding during dragging, and anchor drop impact of a 1-ton Hall's anchor in an experimental basin, the results indicate that under the 3.5 kN anchor dragging impact, the surface of the protection device shows minor damage but remains intact without penetration, ensuring the pipeline remains undamaged. During the anchor overriding during dragging, the protection device demonstrates good stability, effectively safeguarding the pipeline. Even under the equivalent 15-meter water depth anchor drop impact condition, although the protection device sustains some damage, it still maintains its protective function, with no damage to the pipeline. The study confirms that the new type of subsea pipeline protection device exhibits strong resistance to threats such as ship anchor impact, overriding, and drop, providing key technical support and practical evidence for preventing ship anchor damage to subsea pipelines.

## KEYWORDS

Protective Cover, Subsea Pipeline, Anchor Dragging, Anchor Dropping, Prototype Experiment

## 1. INTRODUCTION

Subsea pipelines are crucial "arteries" for offshore oil and gas transportation, often referred to as the "lifelines" of marine oil and gas production systems. Any rupture or leakage can significantly threaten marine environmental safety and resource sustainability. In recent years, various maritime regions in China have witnessed numerous incidents where subsea pipelines have been damaged due to ship anchor dragging and fishing activities, leading to substantial economic losses. To advance research on key technologies for protecting subsea pipelines from anchor-induced damage, we have developed an innovative subsea pipeline protection device, as illustrated in Figure 1. To assess the effectiveness of this protection device against anchor impacts, it is essential to conduct drag anchor impact experiments. The ship anchor system serves as a fundamental component for vessel mooring, offshore platform positioning, and subsea engineering. Therefore, understanding

the movement and force characteristics of the anchor system is crucial for ensuring the safety and integrity of marine operations.

In recent years, physical model tests of drop and dragging have revealed the coupled mechanism of anchor-soil-hydrodynamics through multi-scale experiments and numerical simulations. The ISO 9514 series standards (ISO 9514-1:2006) emphasize that model tests must satisfy both geometric similarity and flow similarity. For instance, Kim et al. (2015) employed a 1:20 scaled sand model and used high-speed cameras and pressure sensors to quantify the nonlinear relationship between anchor claw penetration depth and the soil internal friction angle ( $\varphi$ ). They discovered that for every 1° increase in  $\varphi$ , the soil resistance ( $R_s$ ) rose by approximately 8%. Li & Chen (2020), by combining the discrete element method (DEM) with physical modeling, revealed that under the combined effects of waves and ocean currents, the peak dynamic load on the anchor chain can reach up to 3.2 times the static load. Wang et al.

## Quick Response Code



## Access this article online

Website  
[www.aiem.com.my](http://www.aiem.com.my)

DOI:  
[10.7508/aiem.01.2025.28.34](https://doi.org/10.7508/aiem.01.2025.28.34)



**Figure 1:** Schematic of the Novel Subsea Pipeline Protection System

(2020) developed a fiber-optic sensing system to monitor soil resistance at the anchor-soil interface in real-time, achieving an accuracy of 92%. Koutsouvelis & Sorensen (2006) simulated seismic liquefaction using a shake table and found that after liquefaction, the anchor's residual resistance was only 30% to 50% of its original value. Felippa's (2004) fluid-structure interaction model allows real-time correction of model deviations. Randolph & Gourvenec (2013) established a formula for calculating soil resistance, while Guedes Soares & Godinho (2006) identified soil liquefaction as the dominant failure mode for gravity anchors in deep-water environments, recommending an increase in the safety factor for the anchor's self-weight to 1.8. Chen & Ye (2017) used DEM simulations to study the rotational behavior of screw anchors and found a negative correlation between the spacing of blades and the liquefaction threshold. Yu & Liu (2010) applied machine learning algorithms to reduce noise in measurement data to below 5%. Cundall's (1971) particle flow model uncovered the micro-scale shear mechanisms. Typically, physical model tests of ship anchors use a normal model, with geometric scales ranging from 1:20 to 1:50. However, the scale effects arising from the reduction in model size are still difficult to eliminate. To mitigate the scale effect, this paper proposes a ship anchor impact physical model test method based on prototype dimensions.

## 2. MODEL TESTING METHODOLOGY

### 2.1 Experimental Design

To eliminate the discrepancies arising from scale effects, the physical model must utilize a prototype protection device for the related experiments. The dragging impact tests are conducted within a testing basin measuring 20 meters in length, 9 meters in width, and 2 meters in height, with a 20 cm thick layer of soil placed beneath the protective cover. The ship anchor is arranged on a sliding carriage, which is connected to a variable-speed winch by means of a steel cable. To ensure the sliding carriage moves in alignment with the direction of the water tank, equidistant tracks are installed directly beneath the carriage, as depicted in Figure 2. The experiments will utilize a 1-ton ship anchor (Hall's anchor) for the dragging trials. For medium-sized fishing vessels, which typically carry anchor weights ranging from 0.5 to 1.0 tons, this configuration is capable of meeting the requirements of the vast majority of such vessels. The protective cover is cast as a single unit from fiberglass, with a thickness of 3 cm and an overall mass of 4,900 kg.

### 2.2 Experimental Method

During the experiment, the speed of the dragging anchor is controlled by adjusting the variable frequency power of the winch. A disengagement mechanism is installed at the trailer to prevent collision with the protective cover. The spatial six degrees of freedom position of the protective cover is measured utilizing the principle of electromagnetic positioning. For this purpose, the measurement system employed is the German-manufactured FASTRAK non-contact motion

measurement system, which comprises an electromagnetic transmitter, electromagnetic sensors, a data acquisition device, and acquisition software. This setup provides a non-contact, rigid body motion measurement system capable of tracking six degrees of freedom. The experimental content encompasses the stability of the subsea pipeline protective cover, assessment of damage, and the condition of the subsea pipeline.

### 2.3 Operating Condition Matrices

The relevant operating condition matrices for the prototype ship anchor impact tests on the protective device in the water basin are presented in the Table 1 and Table 2, with the dragging impact locations illustrated in Figure 3.

**Table 1:** Operating Condition Matrixes for Water Basin Tests

Group	Dragging Anchor Contact Position	Dragging Anchor Speed
1	#1	1.5kn
2		2.5kn
3		3.5kn
4	#2	1.5kn
5		2.5kn
6		3.5kn
7	#3	1.5kn
8		2.5kn
9		3.5kn

**Table 2:** Test Matrix for Anchor Drop Scenarios

Matrix	Dragging Anchor Contact Position	Anchor Drop Height	Test Content
1	#1	1.00m	1) Stability of the protective cover
2		1.58m	
3		2.27m	2) Damage to the protective cover 3) Condition of the subsea pipeline

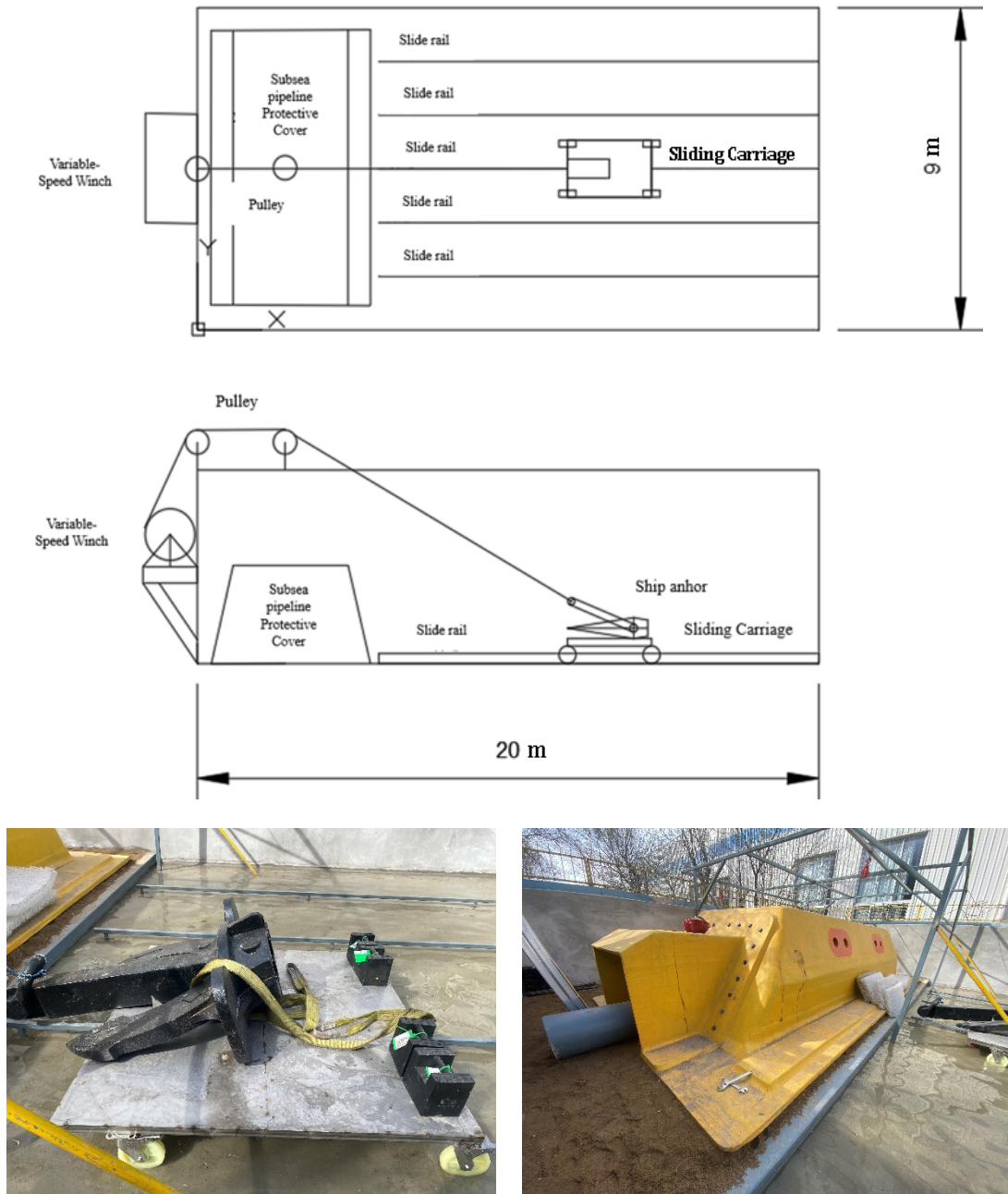


Figure 2: Dragging System and Model Arrangement in the Testing Basin (Unit: meter)



Figure 3: Dragging Anchor Impact Position

### 3. TEST RESULTS

#### 3.1 Dragging Anchor Impact Test Results

The results of the dragging anchor impact tests are presented in Table 3. The anchor, at positions #1 (endpoint), #2 (equidistant point), and #3 (center), impacted the protective cover at speeds of 1.5 kN, 2.5 kN, and 3.5 kN, respectively. After the impact, slight damage occurred on the surface of the protective cover, with damage ranging from 3.5 to 10 cm in size and a depth of less than 1 cm. However, no perforation occurred. The protective cover showed minimal displacement and did not make contact with the subsea pipeline. The subsea pipeline remained intact, as shown in Figure 4.

#### 3.2 Results for Override Test of Dragging Anchors

In order to simulate the process of a dragging anchor overriding the protective cover under the influence of towing force, a crane was used to tow a 1-ton anchor for a climbing test on the surface of the protective cover, as shown in Figure 5. During the test, the anchor overrode the protective cover at three positions: the endpoint (1#), equidistant point (2#), and center (3#). Throughout the test, the protective cover remained stable, with only minor damage to the paint in certain areas of the surface, and no visible scratches were observed. The surface damage was significantly less than that observed in the dragging anchor impact test. The subsea pipeline inside the protective cover remained stable, and the protective cover provided effective protection for the pipeline, as shown in Table 4.

**Table 3: Dragging Anchor Impact Test Results**

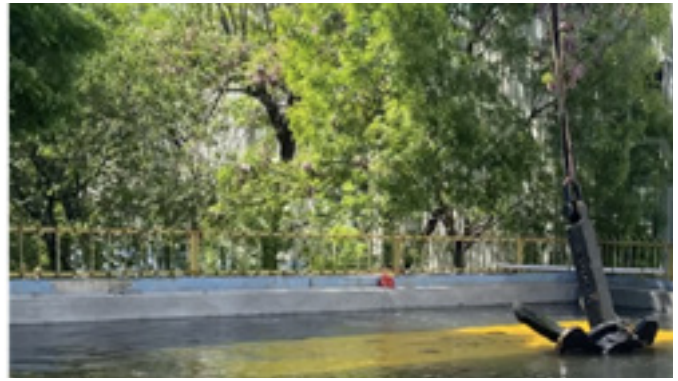
Test Content	Test Condition				Experimental Results
	Position	Direction	Anchor Speed	Dragging Contact Form	
Basin Test of the Prototype Protective Device Against Ship Anchor Impacts	Center	Forward (Most Adverse)	1.5kn/2.5kn/3.5kn	Impact on Protective Cover Base	1) Minor surface damage to the protective cover, no perforation; 2) Minimal displacement of the protective cover, no contact with the subsea pipeline; 3) No impact on protective effectiveness.
	Equidistant Point	Forward (Most Adverse)	1.5kn/2.5kn/3.5kn	Impact on Protective Cover Base	1) Minor surface damage to the protective cover, no perforation; 2) Minimal displacement of the protective cover, no contact with the subsea pipeline; 3) No impact on protective effectiveness.
	Endpoint	Forward (Most Adverse)	1.5kn/2.5kn/3.5kn	Impact on Protective Cover Base	1) Minor surface damage to the protective cover, no perforation; 2) Minimal displacement of the protective cover, no contact with the subsea pipeline; 3) No impact on protective effectiveness.



**Figure 4: Damage of the Protective Cover**



(a) 1# point



(b) 2# point



(c) 3# point

**Figure 5:** Dragging Anchor Override Test on Protective Cover

Table 4: Results for Override Test of Dragging Anchors			
Test Content	Test Condition		Experimental Results
	Position	Direction	
Basin Test of the Prototype Protective Device Against Ship Anchor Override	Center	Forward (Most Adverse)	1) Paint damage on the surface of the protective cover, no visible scratches; 2) Minimal displacement of the protective cover, no contact with the subsea pipeline; 3) Subsea pipeline remained intact.
	Equidistant Point	Forward (Most Adverse)	1) Paint damage on the surface of the protective cover, no visible scratches; 2) Minimal displacement of the protective cover, no contact with the subsea pipeline; 3) Subsea pipeline remained intact.
	Endpoint	Forward (Most Adverse)	1) Paint damage on the surface of the protective cover, no visible scratches; 2) Minimal displacement of the protective cover, no contact with the subsea pipeline; 3) Subsea pipeline remained intact.

**3.3 Anchor Drop Impact Test Results**

The results of the anchor drop impact test at varying heights are presented in Table 5 and Figure 6. It is evident that as the height from which the anchor is dropped increases, both the extent and depth of the damage inflicted on the surface of the protective cover also rise significantly. When the drop height reached 2.27 meters (equivalent to an anchor drop at a depth of 15 meters), the number of layers of the fiber within the protective cover that sustained damage reached 5 to 6, with a penetration depth of up to 1.5 centimeters. Notably, the protective cover was not penetrated by the anchor, and its protective efficacy remained intact, ensuring the subsea pipeline sustained no damage.

**4. CONCLUSION**

Based on the prototype physical model tests conducted under conditions of anchor dragging impact, anchor overriding during dragging, and anchor drop impact with a 1-ton Hall’s anchor, an experimental investigation was carried out on the overall stability, structural damage, and protective effectiveness of the novel subsea pipeline protective cover. The following conclusions were drawn:

- (1) Upon impact with the protective cover at a speed of 3.5 kN, only minimal surface damage occurred, with the damage extent ranging from 3.5 to 10 cm and a depth of less than 1 cm; no perforation was observed.

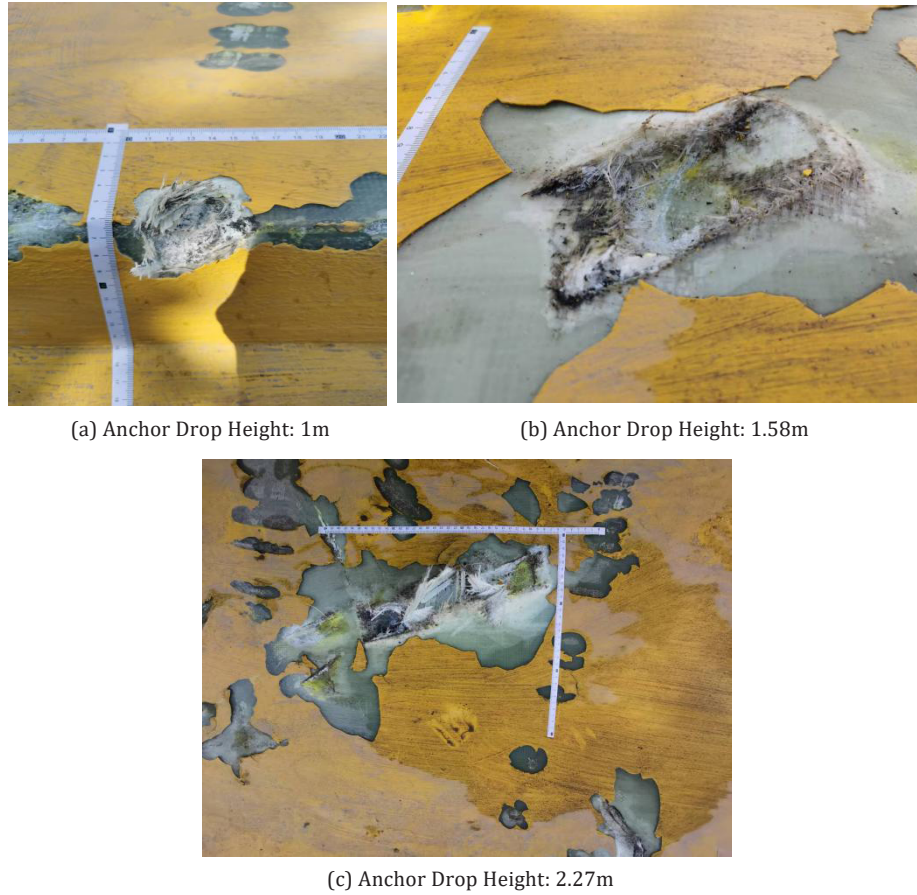


Figure 6: Impact Test Results at Different Anchor Drop Heights

Table 5: Anchor Drop Impact Test Results			
Test Content	Completed Conditions		Experimental Results
	Position	Drop Height	
Protective Device Test Against Ship Anchor Impacts	#1 Drop Point	1.00m	1) Painting damage on the surface of the protective cover, noticeable damage to the fiber layers of the protective cover, no penetration occurred; 2) Protective efficacy remained unaffected.
		1.58m	1) A certain degree of damage to the fiber layers of the protective cover, no penetration occurred; 2) Protective efficacy remained unaffected.
		2.27m	1) Moderate damage to the fiber layers of the protective cover, no penetration occurred; 2) Protective efficacy remained unaffected.

The protective cover exhibited no significant displacement, nor did it contact the subsea pipeline, which remained intact.

(2) During the process of the anchor overriding the protective cover over the subsea pipeline, the cover maintained its stability, with only isolated areas of paint coating exhibiting damage and no significant scratches detected. The internal subsea pipeline remained stable, and the protective cover provided an effective safeguard.

(3) When the anchor drop height reached 2.27 meters (equivalent to dropping from a depth of 15 meters), the fiber layers of the protective cover sustained damage, with 5 to 6 layers affected and a depth of up to 1.5 cm. The protective cover was not breached by the anchor drop, preserving its protective efficacy, and the subsea pipeline remained undamaged.

(4) The novel subsea pipeline protective cover demonstrates excellent resistance to both dragging anchor impacts and anchor drops.

REFERENCES

Chen, Q., & Ye, Z. (2017). Discrete element modeling of anchor-soil interaction. *Journal of Marine Science and Technology*, 22(3), 541–555.

Cundall, P. A. (1971). A computer model for simulating progressive large movements in blocky rock systems. *Geotechnique*, 21(3), 47–65.

Felippa, C. A. (2004). *Finite element procedures*. Butterworth-Heinemann, 345-412.

Guedes Soares, C., & Godinho, L. (2006). Risk assessment of offshore anchoring systems. *Ocean Engineering*, 33(17), 2231–2246.

ISO 9514-1:2006. *Hydraulic models–Vocabulary and general principles*. International Organization for Standardization.

Kim, H. G., Hong, S. P., & Park, J. H. (2015). Numerical and physical modeling of anchor dynamics. *Ocean Engineering*, 106, 246–257.

Koutsouvelis, G., & Sorensen, J. D. (2006). Anchoring systems for offshore structures: A review. *Marine Structures*, 19(5), 401–423.

Li, Z., & Chen, J. (2020). Dynamic response of anchor-chain systems under wave-current interaction. *Marine Structures*, 58, 1-16.

Randolph, M. F., & Gourvenec, S. (2013). Pile bearing capacity in sand. *Geotechnique*, 63(1), 1–21.

Wang, Y., Zhang, L., & Li, X. (2022). Real-time monitoring of anchor-soil interface using fiber-optic sensing. *Sensors*, 22(12), 3895.

Yu, M. F., & Liu, S. J. (2010). Soil-structure interaction in anchoring systems. *Soil Dynamics and Earthquake Engineering*, 30(10), 907–916.

